Signal Processing 84 (2004) 407–420

Autoregressive modeling of the Wigner–Ville distribution based on signal decomposition and modified group delay

Malini. B. Nayak[a,1], S.V. Narasimhan[b,*]

[a] *Department of Electronics and Communication Engineering, National Institute of Technology Karnataka, Surathkal 574157, India*
[b] *Signal Processing and Telemetry Group, Aerospace Electronics and Systems Division, National Aerospace Laboratory, Bangalore 560017, India*

Received 21 June 2001; received in revised form 5 June 2003

Abstract

An autoregressive modeling of the Wigner–Ville distribution (WVD), based on signal decomposition (SD) by a perfect reconstruction filter bank (PRFB) and the modified magnitude group delay function (MMGD), has been proposed. The SD and MMGD, respectively, reduce the existence of crossterms (without any time smoothing) and the Gibb's ripple effect (due to truncation of the WVD kernel, without applying any window), significantly. In view of this, the modeling is not affected by either the crossterms or the Gibb's ripple and the window that would have been used. The proposed method represents actual time–frequency information parsimoniously and compared to the existing WVD modeling methods, its performance is significantly better in terms of both time and frequency resolution (as there is no time and frequency smoothing) and noise immunity/variance and is computationally efficient.

Keywords: Wigner–Ville distribution; Group delay functions; Signal decomposition by perfect reconstruction filter bank and autoregressive modeling

1. Introduction

The Wigner–Ville distribution (WVD) was introduced as a time frequency representation (TFR) for processing the nonstationary signals and to alleviate the tradeoff between time localization and frequency resolution, found in the short-time Fourier transform. The WVD, at any time instant, is the Fourier transform (FT) of the instantaneous autocorrelation (IACR) sequence (WVD kernel) of infinite lag length and hence theoretically, it has infinite resolution both, in time and frequency [1]. However, practically, it is the pseudo WVD (PWVD) that is computed which considers IACR only for a finite number of lags. In the PWVD, to overcome the abrupt truncation effect, the IACR is weighted by a window function and for a given lag length, this *deteriorates the frequency resolution*. The WVD being quadratic in nature, introduces crossterms for a multi-component signal. The crossterm makes the interpretation of the WVD difficult and the crossterms can be reduced by time smoothing, *only at the cost of time resolution*.

* Corresponding author. Tel.: +80-527-3351; fax: +80-527-0670.
E-mail address: svn@css.cmmacs.ernet.in (S.V. Narasimhan).
[1] Presently, at Infineon Technologies India Pvt. Ltd., 10th floor Discoverer Building, International Tech Park, Bangalore 560066, India.

0165-1684/$ - see front matter © 2003 Elsevier B.V. All rights reserved.
doi:10.1016/j.sigpro.2003.11.003

In the last two decades, efforts have been made to: suppress crossterms effectively, improve the frequency resolution and to maintain the desired TFR properties [3]. In Choi–William's distribution, there is a trade-off between crossterm suppression and the frequency resolution. In the cone–kernel [18], the crossterm suppression and the frequency resolution are achieved without much importance for the TFR properties. The reduced interference kernel [3] is an improved version of Choi–Williams distribution.

In the PWVD, the frequency resolution is determined by the lag length considered and the type of the window applied and the time resolution by the degree of time smoothing used, in suppressing the crossterms. Further, TFR by itself involves large amount of data/storage. Hence, it is very much essential: to improve the frequency and time resolution and make the TFR representation efficient. The parametric modeling of the WVD provides, even for few autocorrelation lags, significantly improved frequency resolution and efficient representation. In the parametric modeling of the WVD so far considered [11,15,16], at each time instant, the IACR is autoregressively modeled. The WVD is supposed to represent the power spectrum of the data at each sample instant, however, as the starting point is the WVD kernel, there are attempts to model the kernel than the data and due to the product operation on the signal, the model order required is twice that for the data. Modeling the WVD information was attempted by considering a real WVD kernel [11] obtained by using an input signal sampled at twice the Nyquist sampling rate and for modeling, the kernel is treated as the data. As a symmetrical sequence cannot be generated by an AR process and the WVD kernel being symmetric, modeling WVD information is a problem. This problem has been solved by either modeling the spectrally equivalent nonsymmetrical kernel (SEFKM) [15] or modeling the half kernel (HKM) [16]. In the former, the time smoothed WVD kernel is converted to a spectrally equivalent non-symmetrical real kernel by associating a phase to the magnitude spectrum and the phase is derived from WVD using the real Hilbert transform. To overcome the phase errors due to the Gibb's ripple associated with the WVD, the windowing has been used [15]. Further, for modeling purpose, this real kernel is converted to an analytic one as the order gets halved, for complex signals. In the HKM approach [16], for modeling, the smoothed autocorrelation kernel only for positive lags is treated as an AR process and the negative half is considered as redundant. Since the half kernel is complex, the model order required is also half of that of the real one. However, the use of half kernel, models *the analytic spectrum of the desired spectrum* [2]. In these modeling methods, the residual crossterms after smoothing may affect the model order and the modeled spectrum.

The use of unsmoothed WVD information for modeling, introduces strong spectral peaks corresponding to crossterms and necessitates the use of good degree of time smoothing which however, deteriorates the time resolution of the TFR. Also, as pointed out, windowing the IACR is essential to overcome the phase errors, in deriving the unsymmetrical kernel of equivalent spectral magnitude [15] prior to modeling and this windowing will certainly affect the frequency resolution of the modeled spectrum.

Recently, WVD which uses signal decomposition (SD) realized by a perfect reconstruction filter bank (PRFB) to reduce the existence of cross terms [13], the modified magnitude group delay (MMGD) [8,17] to remove: the ringing effect of the instantaneous power spectrum [5] and the Gibb's ripple for the WVD [7], without using any window function; have been proposed. In the SD, the IACR of the component signals are computed separately and then added to get the IACR of the original signal and this will avoid the interaction between the components. The truncation effect/ringing manifests as zeros close to the unit circle and the MMGD [17] removes these zeros without disturbing the signal poles and hence overcomes the Gibb's ripple/ringing, preserving the frequency resolution of the rectangular window. Also they provide additional noise immunity as the SD removes possible interaction terms between noise components and the MMGD removes the zeros due to noise which are close to unit circle, in addition to removing the zeros due to truncation. Also WVD which uses both, SD to remove crossterm and MMGD to remove Gibb's ripple, has been explored [6,9].

In this paper, an autoregressive modeling of the WVD spectral information which is significantly free from: crossterms without time smoothing due to use of signal decomposition by perfect reconstruction filterbank and Gibb's ripple without any windowing

due to use of the modified magnitude group delay, has been proposed. The modeling is not affected by either the crossterms or the Gibb's ripple and the window that would have been used. The proposed method, represents actual time–frequency information parsimoniously and compared to the existing WVD modeling methods, its performance is significantly better in terms of: both time and frequency resolution and noise immunity/variance and is computationally efficient.

2. Wigner–Ville distribution (WVD) [1]

For a signal $x(t)$, the WVD is defined as

$$W_x(t,\omega)=\int_{-\infty}^{\infty} x(t+\tau/2)x^*(t-\tau/2)\mathrm{e}^{-\mathrm{j}\omega\tau}\,\mathrm{d}\tau, \quad (1)$$

where $r(\tau)=[x(t+\tau/2)x^*(t-\tau/2)]$ is the *instantaneous autocorrelation* function and $*$ indicates conjugate operation. For computational purposes, it is necessary to weigh the signal by a window before evaluating the WVD and this window slides along the time axis with time instant t, where the WVD has to be evaluated. For a window function, $h(t)$, $h(t)=0$ for $|t|>T/2$, the WVD of the windowed signal is

$$\mathrm{PW}_x(t,\omega)=\frac{1}{2\pi}\int_{-\infty}^{\infty} W_x(t,\xi)W_h(t,\omega-\xi)\,\mathrm{d}\xi, \quad (2)$$

where $W_h(t,\omega)$ is the WVD of the window function. This WVD of the windowed signal is called *pseudo Wigner–Ville distribution* (PWVD), $\mathrm{PW}_x(t,\omega)$. The effect of the window is to *smear* the WVD along the frequency axis. For a real symmetrical window,

$$\mathrm{PW}_x(t,\omega)=\int_{-\infty}^{\infty}[x(t+\tau/2)x^*(t-\tau/2)] \times h^2(\tau/2)\mathrm{e}^{-\mathrm{j}\omega\tau}\,\mathrm{d}\tau. \quad (3)$$

Effectively, the PWVD is the FT of the windowed function $[x(t+\tau/2)x^*(t-\tau/2)]$, the window being $h^2(\tau/2)$. The window *eats away* the correlation function at higher lags, which results in poor spectral resolution.

The quadratic operation on the signal, causes the WVD to be a bilinear transformation. For a composite signal with two components, $x(t)=x_1(t)+x_2(t)$ and for $x_1(t)=\mathrm{e}^{\mathrm{j}(\omega_1 t+\phi_1)}$ and $x_2(t)=\mathrm{e}^{\mathrm{j}(\omega_2 t+\phi_2)}$,

$$W_x(t,\omega)=2\pi\left[\delta(\omega-\omega_1)+\delta(\omega-\omega_2) +2\delta\left(\omega-\frac{\omega_1+\omega_2}{2}\right)\cos\{(\omega_1-\omega_2)t +(\phi_1-\phi_2)\}\right].$$

The third term is the crossterm due to interference between the two components. The crossterm appears midway between two components of the signal. Its amplitude is proportional to product of the two components' amplitudes and it oscillates in time, at a frequency equal to the frequency separation between them. The presence of the crossterm poses a major problem in the interpretation of the WVD of a multicomponent signal. As the crossterm oscillates in time, smoothing the WVD in time, attenuates the crossterms and enables a meaningful representation of the signal components, but *only at the cost of time resolution*.

3. Autoregressive modeling of the WVD [11,15,16]

In the PWVD, the frequency resolution is limited by the lag length considered and the type of the window applied and the TFR by itself involves large amount of data/storage, hence it may be required to improve the frequency resolution beyond the limit provided by the rectangular window and also make the TFR efficient. The parametric modeling of the WVD provides significantly improved frequency resolution even for the autocorrelation with few lags and efficient representation.

3.1. Autoregressive modeling

A model offers insight into the structure of the process, such as the number of resonances, and produces a high-resolution spectral estimate in a compact form by a few parameters. A signal $x(n)$ can be represented by a linear predictive AR model as

$$x(n)=e(n)-\sum_{i=1}^{p} a_i^p x(n-i), \quad (4)$$

where p is the order of the model, a_i^p are the AR coefficients and $e(n)$ is error and is supposed to be

white if the order is sufficient. The power spectral density $S_x(\omega)$ of the signal $x(n)$ is given by

$$S_x(\omega) = \frac{\varepsilon_p}{|1 + \sum_{i=1}^{p} a_i^p e^{-j i\omega}|^2}, \quad (5)$$

where $\varepsilon_p = S_e(\omega)$, the power spectral density of the error $e(n)$.

Various methods for extracting the model parameters which are in practice with their relative merits are [4]: autocorrelation or Yule–Walker method, Burg method, covariance method and modified covariance method.

3.2. Spectrally equivalent full kernel modeling of WVD (SEFKM) [15]

The WVD is real due to the complex symmetry of its kernel. Therefore, the WVD can be interpreted as the magnitude of a spectrum, whose phase is unknown. By associating a phase to this magnitude,

$$\bar{W}_x(n,\omega) = W_x(n,\omega) e^{j \arg[\bar{W}_x(n,\omega)]} \quad (6)$$

a nonsymmetrical kernel can be obtained by inverse Fourier transformation of $\bar{W}_x(n,\omega)$, and modeled as an AR process. The phase to be associated can be obtained from

$$\arg[\bar{W}_x(n,\omega)] = \mathrm{HT}[\log(W_x(n,\omega))], \quad (7)$$

where HT stands for Hilbert transform.

In [15], the phase to be associated has been obtained from HT for real signals. However, the WVD does not have the symmetry of a real signal as it is the FT of a conjugate symmetric sequence. In view of this, at each instant of time, a symmetric magnitude spectrum valid for a real signal is derived from the WVD and the phase to be associated is found using the HT for real signals as below,

$$\arg[\bar{W}_x(n,\omega)] = \mathrm{HT}[\log(W_x(n,\omega))].$$

By associating a phase to this magnitude as

$$\bar{W}_x(n,\omega) = W_x(n,\omega) e^{j \arg[\bar{W}_x(n,\omega)]},$$

the spectrally equivalent nonsymmetrical kernel is obtained by the inverse transformation of $\bar{W}_x(n,\omega)$. For logarithmic operation, $W_x(n,\omega)$ should be positive. However, due to crossterms and truncation effects, $W_x(n,\omega)$ may be negative and these are replaced by small positive values and may result in higher model order. Smoothing the WVD in time results in attenuation of crossterms and meaningful modeling. Windowing the IACR improves the accuracy of the phase reconstruction by reducing Gibb's effect due to large sidelobes of the inevitable rectangular window [15].

The nonsymmetric kernel obtained using the real HT is real. Since the modeling a complex nonsymmetric kernel results in a reduction in the model order by a factor of two, the real kernel is converted to a complex analytic signal. The kernel modeling has been done by modified covariance method.

In this method, the windowing of the WVD kernel for Gibb's ripple reduction to get accurate phase, time smoothing to overcome crossterm effect result in the deterioration in frequency and time resolution, respectively. Furthermore, the use of real HT three times (getting the analytic signal for WVD, to get the real nonsymmetric kernel in getting the phase and converting the real nonsymmetric kernel to a complex one) increases the computational load.

3.3. Half kernel modeling of WVD (HKM) [16]

In overcoming the drawbacks of the SEFKM and specifically, to take advantage of modeling the complex kernel which reduces model order by a factor of two, the half kernel was introduced. As a symmetric kernel cannot be modeled, this approach avoids potential symmetry problems by considering only half of the complex WVD kernel, i.e., for positive lags and neglecting the other half for negative lags, as redundant [16].

Modeling only half of the complex WVD kernel is given by

$$r(n,k) = e(k) - \sum_{i=1}^{p} a_i r(n, k-i), \quad (8)$$

where k varies between 0 and L, instead of $-L$ to L, p is the order of the AR model, a_i's are the coefficients of the AR model, and $e(k)$ is the error.

As compared to SEFKM, since the half kernel which is complex is directly modeled, it is computationally efficient and as the kernel windowing is not involved, its frequency resolution is better.

Here also, to avoid crossterm effects time smoothing WVD kernel is required and this reduces the time resolution.

The spectrum obtained by modeling the half kernel sequence is the analytic spectrum [2] of the full kernel sequence. That is,

$$[E(n,\omega)]^2 = \left|\tfrac{1}{2}(W_x(n,\omega) + \mathrm{j}\bar{W}_x(n,\omega))\right|^2,$$

where $\bar{W}_x(n,\omega)$ is the Hilbert transform of $W_x(n,\omega)$ and $W_x(n,\omega)$ is the smoothed Wigner–Ville distribution. Thus, the half kernel does not model the desired time varying WVD spectrum.

Due to the large dynamic range of the spectra, the envelope $E(n,\omega)$ strongly enhances the highest power frequency bands with respect to $W_x(n,\omega)$. Consequently, the noise components lying outside the enhanced frequency bands are largely attenuated in $E(n,\omega)$ with respect to $W_x(n,\omega)$, and thus, $E(n,\omega)$ is more robust to broadband noise than $W_x(n,\omega)$.

4. The improved WVD (IWVD)

The multicomponent signal is decomposed into its components by perfect reconstruction filter bank and the IACR of the individual components are computed and added to get the IACR of the original signal. Further, this IACR significantly free from crossterms, is subjected to MMGD for removing the Gibb's ripple, without applying any window function.

4.1. Signal decomposition by perfect reconstruction filter bank [13]

The impulse response of the subfilters of a uniform filter bank are obtained by complex modulation of a low-pass filter and is given by

$$h_i(n) = h(n)\mathrm{e}^{\mathrm{j}\omega_i n}, \tag{9}$$

where

$$h(n) = \frac{1}{M}\,\frac{\sin(n\pi/M)}{n\pi/M} \quad \text{and}$$

$$\omega_i = 2\pi(i-1)/M, \quad i = 1, \Lambda, M,$$

$h(n)$ is the impulse response of a prototype low-pass filter and M is the number of subfilters. Thus, the transfer function of the subfilters is

$$H_i(\omega) = H(\omega - \omega_i), \quad i = 1, \Lambda, M.$$

The output from the ith subfilter is

$$z_i(n) = x(n) \otimes h_i(n), \quad \otimes\text{: convolution.}$$

The complex signal $z_i(n)$ becomes analytic, provided the Fourier transform of $z_i(n)$, $Z_i(\omega) = 0$ for $\omega < 0$. This will occur for all subfilters if $H(\omega) = 0$ for $|\omega| > \pi/M$. To achieve this, the real input $x(n)$ to the filter bank is band-limited to the frequency interval $\{\pi/M,\ \pi - \pi/M\}$ [13]. Thus, the spectrum of $x(n)$ is covered by the subfilters indexed $i = 2, \Lambda, M/2$.

For a perfect reconstruction, $h(n)$ should satisfy,

$$h(0) = 1/M,$$

$$h(mM) = 0, \quad \forall m \neq 0, \tag{10}$$

which, in the frequency domain, corresponds to

$$\sum_{i=1}^{M} |H(\omega - \omega_i)| = 1, \quad 0 \leqslant \omega \leqslant 2\pi. \tag{11}$$

To reduce the occurrence of crossterms due to the quadratic nature of the WVD, the multicomponent signal is decomposed into its components using the PRFB discussed, and the individual IACRs of these components are computed and then added to get the complete IACR of the original signal [13]. The IACR of the original signal $r(n,k)$ at nth instant and for lag k is,

$$r(n,k) = \sum_{i=2}^{M/2} r_i(n,k) \tag{12}$$

$r_i(n,k)$ is the IACR of the ith component of the signal.

In the PRFB, if the signal is confined to the frequency interval $\{\pi/M,\ \pi - \pi/M\}$, the filter bank directly generates the required analytic signal for the WVD and the computation of the Hilbert transform of the signal is avoided. Since the filterbank is a perfect reconstruction one, the signal decomposition prior to computation of the WVD kernel does not introduce any errors in the performance of the WVD.

4.2. Modified magnitude group delay (MMGD) and the WVD [5–7,17]

If $x(n)$ is a minimum phase complex signal,

$$\ln|X(\omega)| = \sum_{n=0}^{\infty} [c_{\mathrm{R}}(n)\cos\omega n + c_{\mathrm{I}}(n)\sin\omega n], \tag{13}$$

$$\theta(\omega) = \sum_{n=0}^{\infty} [-c_{\mathrm{R}}(n)\sin\omega n + c_{\mathrm{I}}(n)\cos\omega n], \tag{14}$$

$\theta(\omega)$ is the unwrapped phase and $c(n) = c_{\mathrm{R}}(n) + \mathrm{j}c_{\mathrm{I}}(n)$ are cepstral coefficients. R and I refer to the real and

imaginary parts. For a minimum phase signal, the log-magnitude spectrum and the phase are related by a single set of cepstral coefficients. The GD $\tau_{\mathrm{m}}(\omega)$ is given by

$$\tau_{\mathrm{m}}(\omega) = \frac{-\partial\theta(\omega)}{\partial\omega} = \sum_{n=0}^{\infty} nc_{\mathrm{R}}(n)\cos\omega n + nc_{\mathrm{I}}(n)\sin\omega n = (\tfrac{1}{2})\mathrm{FT}[nc(n) - nc^{*}(-n)]. \quad (15)$$

If $nc(n)$ is conjugate symmetric, $\tau_{\mathrm{m}}(\omega)$ is the Fourier transform of $nc(n)$. Since $c(n)$ sequence is derived from the magnitude, $\tau_{\mathrm{m}}(\omega)$ is called as the magnitude GD for a complex signal (MGD).

In spectral estimation, the goal of achieving a lower variance and a high resolution is to capture a consistent spectral envelope and discard the fine structure without affecting the former. The fine structure/variance is due to: signal truncation effect or associated white noise or due to input white noise that drives a system in generating the signal or any of these combinations. These introduce zeros close to the unit circle and it is these zeros which manifest as spikes, in the GD, contribute significantly to the fine structure of the spectrum and their effect cannot be removed by normal smoothing without the loss of frequency resolution. The periodogram has good frequency resolution, low bias and good signal detectability even at high noise levels, but its variance is large. For a given length of data, averaging of the periodogram or windowed periodogram, or smoothed GD, results in a reduced variance but only at the expense of frequency resolution. The modification suggested in [17] removes these zeros close to the unit circle and hence the spikes effectively, without disturbing the signal/system poles, i.e., without sacrificing the frequency resolution.

The modification basically considers the signal to be characterized by, a transfer function having only the denominator polynomial, generally known as an all pole model and in such a case, the input driving noise to the transfer function or the associated noise with the signal or the truncation effect (zeros) on the signal, corresponds to the numerator. The undesired effect of the numerator, viz., large variance, is removed by dividing the transfer function by the numerator estimate, without significantly disturbing the denominator. The GD domain provides a platform to do this operation, without any singularity problems, as it involves only multiplication and no division. Whereas, the conventional approach of averaging of the periodogram of variance reduction, involves data segmentation and or windowing, not only reduces the variance/effect of the numerator, but also the frequency resolution of the spectral peaks as it pulls the signal poles towards the origin in addition to the zeros (which are close to the unit circle).

If $x(n)$ is a complex signal: generated by an all-pole system, driven by a white noise or has sinusoids with white noise and further, if its spectrum $X(\omega) = N(\omega)/D(\omega)$, $D(\omega)$ corresponds to the system or sinusoids and $N(\omega)$ to the excitation or the associated noise. For this case, the MGD is

$$\tau_{\mathrm{m}}(\omega) = \tau_{\mathrm{m}N}(\omega) - \tau_{\mathrm{m}D}(\omega)$$

$\tau_{\mathrm{m}N}(\omega)$ and $\tau_{\mathrm{m}D}(\omega)$ are the MGDs for $N(\omega)$ and $D(\omega)$, respectively. Also, $\tau_{\mathrm{m}}(\omega)$ is given by

$$\tau_{\mathrm{m}}(\omega) = \frac{X_{\mathrm{m}R}(\omega)Y_{\mathrm{m}R}(\omega) + X_{\mathrm{m}I}(\omega)Y_{\mathrm{m}I}(\omega)}{|X(\omega)|^2} \quad (16)$$

$X_{\mathrm{m}}(\omega) = \mathrm{FT}[x_{\mathrm{m}}(n)]$, $Y_{\mathrm{m}}(\omega) = \mathrm{FT}[y_{\mathrm{m}}(n)]$ and $y_{\mathrm{m}}(n) = nx_{\mathrm{m}}(n)$, $x_{\mathrm{m}}(n)$ is the minimum phase equivalent of $x(n)$.

Also,

$$\tau_{\mathrm{m}}(\omega) = \frac{\alpha_N(\omega)}{|N(\omega)|^2} - \frac{\alpha_D(\omega)}{|D(\omega)|^2}. \quad (17)$$

$\alpha_N(\omega)$ and $\alpha_D(\omega)$ are the numerator of the above Eq. (16) for $\tau_{\mathrm{m}N}(\omega)$ and $\tau_{\mathrm{m}D}(\omega)$, respectively.

The $\tau_{\mathrm{m}N}(\omega)$ will have large amplitude spikes due to very small values of $|N(\omega)|^2$ near the zeros which are close to unit circle and this is not so with the $\tau_{\mathrm{m}D}(\omega)$, as the roots of $D(\omega)$ are well within the unit circle. Hence, in $\tau_{\mathrm{m}}(\omega)$, the effect of excitation or the associated noise masks the system or the signal component which is assumed to be an all-pole one. The effect of these zeros could be reduced by multiplying $\tau_{\mathrm{m}}(\omega)$ by $|N(\omega)|^2$. Also, as the envelope of $|N(\omega)|^2$ is nearly flat, the significant features of $\tau_{\mathrm{m}D}(\omega)$ continue to exist, with the $|N(\omega)|^2$ fluctuations superimposed on it. Hence, the modified MGD (MMGD) $\tau_{\mathrm{mo}}(\omega)$, is

$$\tau_{\mathrm{mo}}(\omega) = \tau_{\mathrm{m}}(\omega)|N(\omega)|^2. \quad (18)$$

The estimate of $|N(\omega)|^2$,

$$|\tilde{N}(\omega)|^2 = |X(\omega)|^2/|\bar{X}(\omega)|^2,$$

$|\bar{X}(\omega)|^2$ is the smoothed power spectrum obtained by the truncated cepstral sequence.

To remove the Gibb's ripple of the WVD due to abrupt truncation of the IACR, without using any window function, the IACR $r(n,k)$ that is significantly free from crossterms, will be subjected to MMGD for a complex signal, since the IACR of a WVD is complex.

In the MMGD, the numerator estimate is

$$\tilde{N}(\omega) = \frac{X(\omega)}{\bar{X}(\omega)} = \left[1 + \frac{\Delta(\omega)}{\bar{X}(\omega)}\right].$$

Here, $\Delta(\omega)$ represents the fluctuating part of $X(\omega)$. For a signal having a *flat spectral* characteristic, in the GD $\tau_{\mathrm{m}}(\omega)$, the contribution is only due to $\Delta(\omega)$. A $\tau_{\mathrm{mo}}(\omega)$, free from fluctuations, is given by [5,7]

$$\tau_{\mathrm{mo}}(\omega) = \tau_{\mathrm{m}}(\omega)|\Delta(\omega)|^2. \tag{19}$$

Presently, for the WVD, it is required to remove the ripple on the floor, which is equivalent to a flat spectral characteristic. $\tau_{\mathrm{m}}(\omega)$ is derived from the FT of the cross term free IACR (using Eqs. (13) and (15)). Though the FT of IACR represents the instantaneous power spectral density (PSD), which is supposed to be a positive quantity at each frequency bin, it may not be so due to the fact that the PSD gets convolved with the FT of the rectangular window (whose presence is inevitable). Since computation of $\tau_{\mathrm{m}}(\omega)$ involves logarithmic operation, it is necessary to ensure that FT of IACR is positive and this is achieved by raising the floor level by scaling up the IACR at the zeroth lag [14], sufficiently and the equivalent magnitude spectrum is obtained from positivity ensured PSD. Further, the linearly weighted cepstral coefficient sequence is made conjugate symmetric [8].

At each time instant, the spectrum that is free from the crossterm, ripple effect, and that has a better frequency and time resolution, is obtained from $\tau_{\mathrm{mo}}(\omega)$ (Eq. (19)) by retracing the MMGD computation procedure in the reverse order. Here, the cepstral coefficient sequence derived from $\tau_{\mathrm{mo}}(\omega)$, has to be made conjugate symmetric. For each TFR slice obtained by the MMGD, the original floor level is restored by subtracting the mean value and adding the scaled mean value.

Since the signal decomposition not only reduces the interaction between signal components but also for the noisy components, it avoids crossterms due to noise and hence has a better noise immunity. Further, MMGD, not only removes the zeros due to ripple effect but also those due to noise and hence provides additional immunity to noise. Hence, the WVD which is based on signal decomposition and MMGD [6], is expected to have improved noise immunity.

4.3. Derivation of the kernel from improved WVD slice for AR modeling

The crossterm and Gibb's ripple free WVD spectrum obtained by the SD and MMGD, respectively, will be modeled. For modeling purpose, from this improved WVD spectrum, a nonsymmetric kernel will be directly derived, using *complex Hilbert transform* [12].

Hilbert transform relates the real and imaginary parts of the FT $X(\omega)$ of a causal sequence $x(n)$. For complex sequence $x(n)$,

$$X_{\mathrm{R}}(\omega) = \mathrm{DFT}[\mathrm{sgn}(n)\,\mathrm{IDFT}[\mathrm{j}X_{\mathrm{I}}(\omega)]] + x_{\mathrm{R}}(0) \tag{20}$$

and

$$X_{\mathrm{I}}(\omega) = -\mathrm{j}\,\mathrm{DFT}[\mathrm{sgn}(n)\,\mathrm{IDFT}[X_{\mathrm{R}}(\omega)]] + x_{\mathrm{I}}(0). \tag{21}$$

For length N,

$$\mathrm{sgn}(n) = \begin{cases} 0, & n = 0,\ N/2, \\ 1, & 0 < n < N/2, \\ -1, & N/2 < n < N. \end{cases}$$

For a minimum phase sequence $x(n)$, it also relates the log-magnitude and phase of $X(\omega)$, i.e., $\ln|X(\omega)|$ and $\mathrm{j}\theta(\omega)$ can be related as

$$\ln|X(\omega)| = \mathrm{DFT}[\mathrm{sgn}(n)\,\mathrm{IDFT}[\mathrm{j}\theta(\omega)]] + c_{\mathrm{R}}(0) \tag{22}$$

and

$$\mathrm{j}\theta(\omega) = \mathrm{DFT}[\mathrm{sgn}(n)\,\mathrm{IDFT}[\ln|X(\omega)|]] + c_{\mathrm{I}}(0), \tag{23}$$

where, $c(n) = c_{\mathrm{R}}(n) + \mathrm{j}c_{\mathrm{I}}(n)$ are the complex cepstral coefficients. That is, given a discrete sequence $x(n)$, the magnitude and phase of its FT $X(\omega)$ can be obtained from each other. Also, a mixed phase complex signal can be converted to a minimum phase equivalent complex signal having the same magnitude function as that of the mixed phase signal, using Eq. (23).

Similar to the existing methods, by associating a phase (Eq. (7)) to $W_x(n,\omega)$ (Eq. (6)), a nonsymmetrical spectrally equivalent kernel can be obtained by taking the inverse FT of $\bar{W}_x(n,\omega)$ and can be modeled as an AR process/signal. However, due to the product operation on the signal, the order of the model required is twice that of the actual input data and this can be avoided by considering the square root of $W_x(n,\omega)$. That is,

$$\bar{W}_x(n,\omega) = [W_x(n,\omega)]^{1/2} e^{j \arg[\bar{W}_x(n,\omega)]}. \tag{24}$$

This results in a nonsymmetrical kernel having spectral magnitude that of the signal and the phase to be associated can be obtained from

$$\arg[\bar{W}_x(n,\omega)] = \mathrm{HT}[\log([W_x(n,\omega)]^{1/2})], \tag{25}$$

where HT is the Hilbert transform for a complex signal.

Unlike the existing methods [15,16], the proposed method is not affected by crossterms as they will not exist due to SD realized by PRFB. Since no time smoothing is required, its time resolution will be significantly better. The SD not only overcomes the crossterms due to signal components but also those due to noise components and hence it improves the noise immunity of the new WVD. Further, unlike the SEFKM, in the new method as the Gibb's ripple is removed by the MMGD *without applying any window*, its frequency resolution is better. This is because, the *window affects the basic WVD autocorrelation kernel itself and a modeling based on it cannot provide correct WVD spectral information*. The MMGD provides additional noise immunity as it removes the zeros close to the unit circle not only due to Gibb's ripple but also those due to noise. Further, the use of HT for a complex signal, in computing the phase, minimizes the computation. Though the HKM does not compute the phase and considers only the WVD kernel for positive lags, it models only the *analytic power spectrum rather than the desired power spectrum of the signal*. However, this is not so with the proposed one. For the existing methods, the order of the model required may be more than that of the proposed method, as they model the product signal rather than the signal itself.

5. Simulation results

The performance of the proposed WVD (IWVD) for two sets of frequencies is illustrated for sinusoidal signal with two components, in the presence of noise. Also, the performance of the proposed method is compared with those of: HKM and SEFKM. In all the examples, number of lags considered is 33. Further, discrete Fourier transform of length 128, is used, in all the cases. The smoothed WVD kernel is achieved by using a boxcar smoothing of 11-points. In this study, modified covariance technique [4] which gives statistically stable spectrum estimates with high resolution is used and the model order used is four. For the SEFKM, no window function is used, in the present study.

For signal decomposition, PRFB consisting of six subfilters are used. The prototype low-pass filter is designed by window method using Kaiser function with a smoothing factor of eight and the filter impulse response being 128. All the other filters of the uniform PRFB are derived by complex modulation of the prototype filter about the center frequency and are *marginally* (*or non*) *overlapping filters*.

In the methods where filterbank is not employed, for the WVD, the analytic signal is derived using the Hilbert transform realised by time domain convolution. But for the proposed method, analytic signals are derived by considering outputs of subfilters indexed from 2 to $M/2$, i.e., 2 and 3 only.

For MMGD, first 16-cepstral coefficients are used in computing the smoothed PSD for the estimation of $|\Delta(\omega)|^2$. To avoid the negative spectral values in the PSD, WVD kernel at zeroth lag has been lifted by a factor of 100.

The time frequency distribution plot, contour plot and the frequency histogram are used to bring out the comparative performance. Further, the performance is quantified by the total frequency estimation error [16], given by $\log_{10}(e_t)$.

$$e_t = \frac{1}{Q}\sum_{j=1}^{Q}\frac{1}{K}\sum_{n=0}^{K}(\hat{f}_{nj} - f_j)^2,$$

where Q is the number of signal components, K is the number of trials, f_j is the actual jth component, and $\hat{f}_{nj}$ is the estimated jth component, in the nth trial.

For the two sinusoids at frequencies 1000 and 2500 Hz with white Gaussian noise at signal-to-noise ratio (SNR) of −5 dB, the results are shown in Fig. 1. (The spectral peaks occur at twice the actual frequencies due to WVD being implemented by fast Fourier transform.) Also the SNR in dB is defined as

$$(\mathrm{SNR})_{\mathrm{dB}} = 10\log 10[\sigma_s^2/\sigma_v^2], \quad \sigma_s^2 = \sum_{n=0}^{L-1} S^2(n),$$

$$\sigma_v^2 = \sum_{n=0}^{L-1} v^2(n)$$

$s(n)$ and $v(n)$ are desired signal and noise components of the signal $x(n)$ considered.

For HKM (Fig. 1(a)) the TFR appears to be very noisy as the peaks are pulled over a wider region and are of different magnitudes. Also, some ridge type effect is also seen. Hence the two peaks are not well separated or resolved. In case of SEFKM (Fig. 1(b)) the TFR is less noisy and the spectral peaks are relatively separated and aligned and are of similar magnitude. For the proposed method, the TFR (Fig. 1(c)) is least noisy as the spectral peaks are significantly concentrated, aligned and hence are well resolved and are of almost same magnitude. The resolvability of the spectral peaks and the variance of the peak location brought out by the contour (Figs. 1(d)–(f)) and histogram (Figs. 1(g)–(i)) plots.

At SNR = −3 and 0 dB, the three methods have a similar performance and the proposed method appears to be better in terms of variance of the spectral peak location.

Fig. 2 illustrates the performance comparison of the three methods for sum of two closely spaced sinusoidal components with frequencies 1750 and 2250 Hz, in the presence of Gaussian white noise, SNR = 0 dB. As seen from the TFR, contour and histogram plots, HKM (Figs. 2(a), (d) and (g)), SEFKM (Figs. 2(b), (e) and (h)) are very poor in resolving the two peaks as they appear to be merged. But the proposed method (Figs. 2(c), (f) and (i)) resolves the peaks as they are well separated. Also, the proposed method exhibits comparatively less spread.

The spectral frequency estimation error listed in Table 1 supports the above results and particularly, for the two closely spaced sinusoids at 0 dB, compared to the other two methods, this error is relatively small for the proposed method.

A sinusoidal signal whose frequency is varied as a sinusoidal function of time is considered to bring out the performance of the proposed method for a nonstationary signal with nonlinear frequency variation and such a study may find application in situations like analysis of nonstationary cardiovascular time series [10]. This has been studied both for a signal with high (20 dB) and low (5 dB) SNRs. It has been found that at high SNR, the proposed method is very effective (Fig. 3) in suppressing the Gibbs ripple, crossterms and providing data compression by modeling. The modeling helps in removing the discontinuities in the contour plots Figs. 3(g) and (h) compared to the Figs. 3(e) and (f). In Figs. 3(h), the width of the contour is narrower than in Figs. 3(e)–(g) and hence the proposed method (SD with MMGD and modeling) gives a better frequency resolution than that of SD (filter bank), SD with MMGD and only SD with modeling. But at low SNRs, (Fig. 4) though the Gibbs ripple and crossterms are suppressed by the MMGD and SD using perfect reconstruction filter bank, the AR modeling gets affected by the residual-noise and hence spectral peak gets broadened (Fig. 4(h)) resulting in a frequency resolution which is poorer than that of without modeling (Fig. 4(f)). Even here, the proposed method has a better frequency resolution than that of SD by filter bank and modeling (Fig. 4(g)). Similar results have been observed even with crossing linear chirp signals.

With the proposed IWVD method, the crossterms, not only due to the signal but also due to the noise, are not allowed to exist significantly, due to signal decomposition prior to computing the WVD kernel. This provides a higher noise immunity and preserves time resolution of WVD. The modeling is not affected by residual crossterms and may not require higher order. Further, the MMGD provides the phase accuracy, as it removes the Gibb's ripple due to abrupt truncation without the use of any window function and hence preserves the frequency resolution of the rectangular window, which further enhances the frequency resolution for modeling. As the MMGD not only removes the zeros due to Gibb's ripple but also those due to

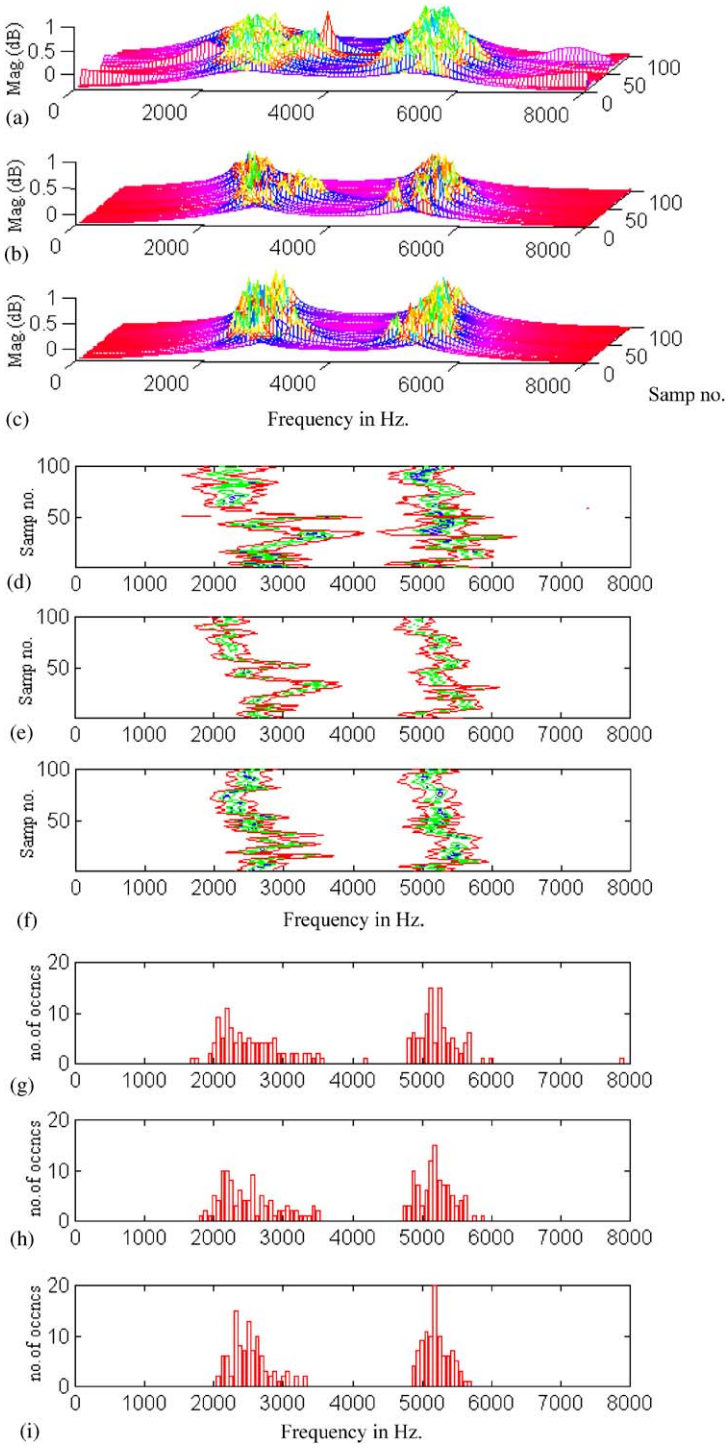

Fig. 1. (a)–(c) TFR for two sinusoids at 1000 and 2500 Hz (SNR = −5 dB) by (a) HKM, (b) SEFKM, and (c) IWVD, (d)–(f) contour plots for (a)–(c), (g)–(i) histogram plots of (a)–(c).

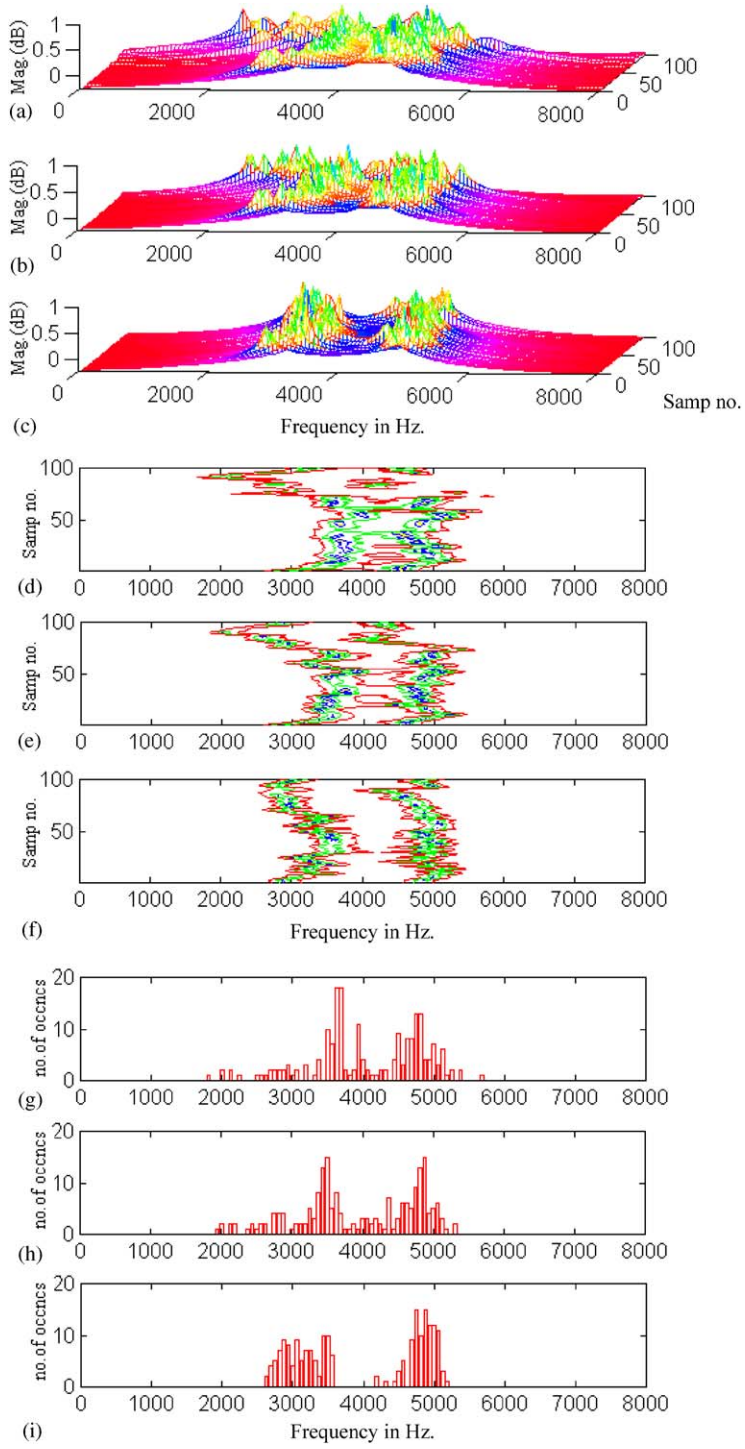

Fig. 2. (a)–(c) TFR for two sinusoids at 1750 and 2250 Hz (SNR = 0 dB) by (a) HKM, (b) SEFKM, and (c) IWVD, (d)–(f) contour plots for (a)–(c), (g)–(i) histogram plots of (a)–(c).

Table 1
Spectral frequency estimation error

Example (Hz)	SNR (dB)	HKM	SEFKM	IWVD
1000 & 2500	0	0.0057	0.0058	0.0127
	−3	0.0269	0.0240	0.0288
	−5	0.0580	0.0558	0.0445
1750 & 2250	0	0.0140	0.0156	0.0123

noise, it further enhances the noise immunity. In view of these, the proposed method, provides better time and frequency resolutions and noise immunity and presents the TFR information, in a efficient way when the SNR is sufficiently high. The use of complex HT reduces the number of computations, which otherwise would have been higher.

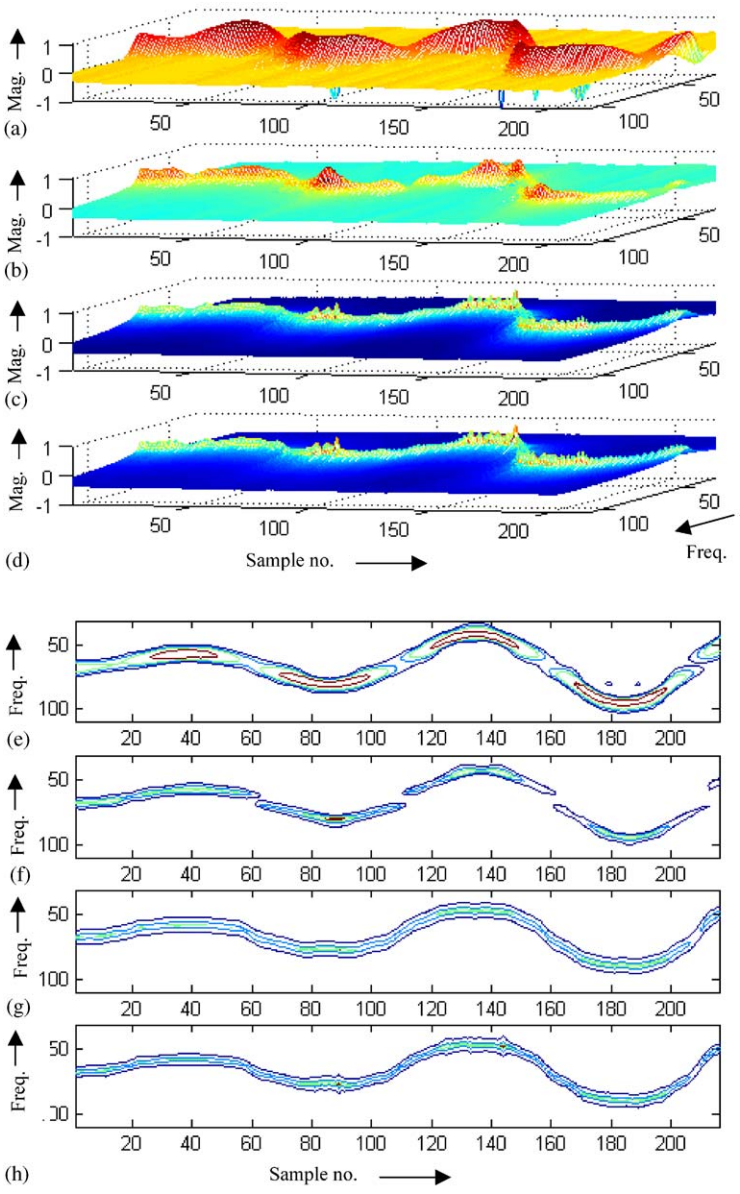

Fig. 3. TFR for a nonstationary signal, SNR = 20 dB by (a) filter bank (FB), (b) FB and MGD, (c) FB and modeling and (d) FB, MGD and modeling, (e)–(h) contour plots for (a)–(d), respectively.

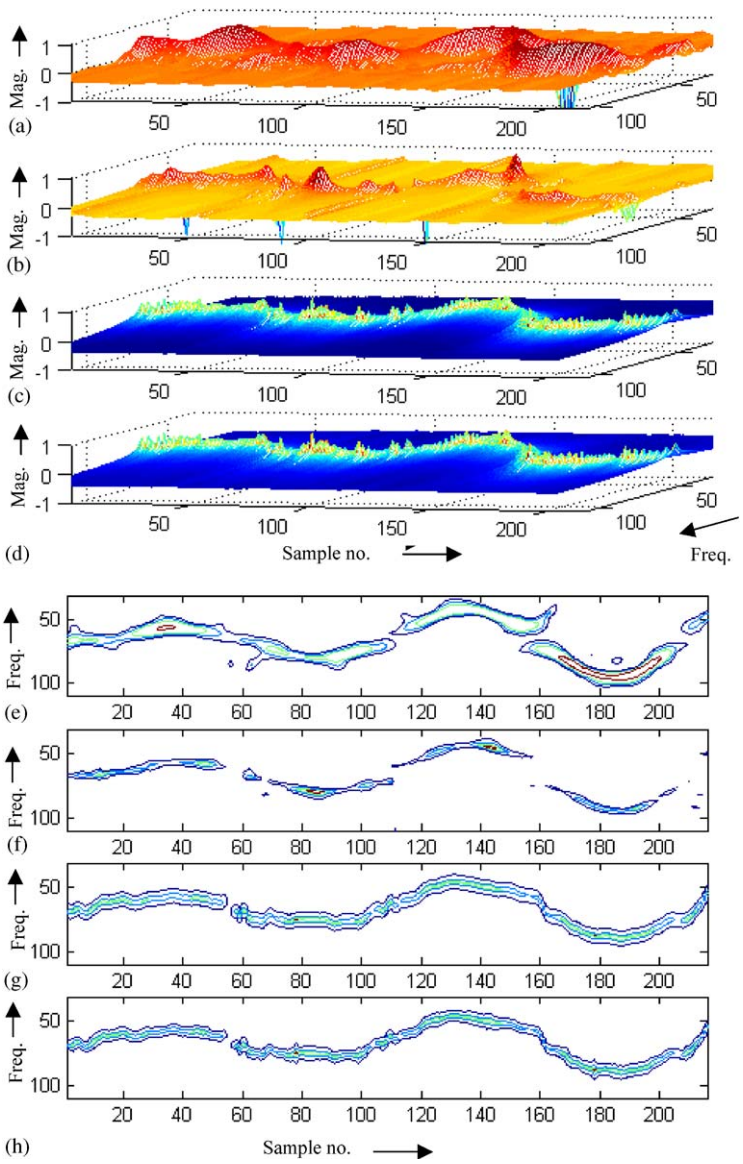

Fig. 4. TFR for a nonstationary signal (SNR = 5 dB) by (a) filter bank (FB), (b) FB and MGD, (c) FB and modeling and (d) FB, MGD and modeling, (e)–(h) contour plots for (a)–(d), respectively.

6. Conclusions

An autoregressive modeling of the Wigner–Ville distribution (WVD), based on signal decomposition (SD) by a perfect reconstruction filter bank (PRFB) and the modified magnitude group delay function (MMGD), was proposed. The SD and MMGD, respectively, significantly reduce the existence of crossterms and the Gibb's ripple effect due to truncation of the WVD kernel, without applying any window. Either the crossterms or the Gibb's ripple and the window that would have been used, do not affect the modeling. The proposed method, represents actual time–frequency information parsimoniously and

compared to HKM and SEFKM methods, its performance was found to be significantly better in terms of: both time and frequency resolution (as there is no time and frequency smoothing) and noise immunity/variance and is also computationally efficient.

References

[1] L. Cohen, Time–frequency distribution—a review, Proc. IEEE 77 (1989) 941–981.
[2] J. Hernando, C. Nadeu, Linear prediction of the one-sided autocorrelation sequence for noisy speech recognition, IEEE Trans. Speech Audio Process. 5 (1) (January 1997) 80–84.
[3] J. Jeong, W.J. Williams, Kernel design for reduced interference distributions, IEEE Trans. Signal Process. 40 (2) (1992) 402–412.
[4] L. Marple, A new autoregressive spectrum analysis algorithm, IEEE Trans. Acoust. Speech Signal Process. 28 (August 1980) 293–306.
[5] S.V. Narasimhan, Improved instantaneous power spectrum (IPS) performance: a group delay approach, Signal Processing 80 (2000) 75–88.
[6] S.V. Narasimhan, M.B. Nayak, Improved Wigner–Ville distribution performance by signal decomposition and modified group delay, Proceedings of International Conference on Communication, Control and Signal Processing (CCSP-2000), Bangalore, India, July 26–28, 2000, pp. 35–39.
[7] S.V. Narasimhan, E.I. Plotkin, M.N.S. Swamy, Power spectrum estimation of complex signals and its application to Wigner–Ville distribution: a group delay approach, Sadhana, (published by Indian Academy of Sciences, India) (Part 1) 23 (1998) 57–71.
[8] S.V. Narasimhan, E.I. Plotkin, M.N.S. Swamy, Power spectrum estimation of complex signals: group delay approach, Electron. Lett. 35 (25) (December 1999) 2182–2184.
[9] M.B. Nayak, Improved Wigner–Ville distribution by signal decomposition, modified group delay and modeling, M.Tech Thesis, Karnataka Regional Engineering College, Surathkal, India, August 2000.
[10] S. Pola, A. Macerata, M. Emdin, C. Marchesi, Estimation of the power spectral density in non-stationary cardiovascular time series: assessing the role of the time–frequency representation (TFR), IEEE Trans. Biomed. Eng. 43 (1996) 46–59.
[11] P.A. Ramamoorthy, V.K. Iyer, Y. Ploysongsang, Autoregressive modeling of the Wigner spectrum, Proceedings of the International Conference on Acoustics Speech and Signal Processing, Dallas, TX, April 1987, pp. 1509–1512.
[12] G.R. Reddy, M.N.S. Swamy, Hilbert transform relations for complex signals, Signal Processing 22 (2) (February 1991) 215–219.
[13] F. Sattar, G. Salomonsson, The use of a filter bank and the Wigner–Ville distribution for time–frequency representation, IEEE Trans. Signal Process. 47 (1999) 1776–1783.
[14] P.P. Vaidyanathan, Mutirate Systems and Filter Banks, Prentice-Hall Inc., Englewood Cliffs, NJ, 1993, pp. 59–60 (Chapter 3, Section 3.2.5, Spectral factorization).
[15] E.F. Velez, R.G. Absher, Smoothed Wigner–Ville parametric modeling for the analysis of nonstationary signals, Proceedings of the IEEE International Symposium on Circuits and Systems, Portland, OK, May 1989, pp. 507–510.
[16] E.F. Velez, R.G. Absher, Parametric modeling of the Wigner half kernel and its application to spectral estimation, Signal Processing 26 (2) (February 1992) 161–175.
[17] B. Yegnanarayana, H.A. Murthy, Significance of group delay functions in spectral estimation, IEEE Trans. Signal Process. 40 (9) (1992) 2281–2289.
[18] Y. Zhao, L. Atlas, R. Marks II, The use of cone shaped kernels for generalized time–frequency representation of nonstationary signals, IEEE Trans. Signal Process. 38 (7) (1990) 1084–1091.